Construction and Building Materials 162 (2018) 674–682

Contents lists available at ScienceDirect

Construction and Building Materials

journal homepage: www.elsevier.com/locate/conbuildmat

Investigating the effects of maximum aggregate size on self-compacting steel fiber reinforced concrete fracture parameters

Mohammad Ghasemi, Mohammad Reza Ghasemi *, Seyed Roohollah Mousavi

Civil Engineering Department, University of Sistan and Baluchestan, Zahedan, Iran

HIGHLIGHTS

- The effects of maximum aggregate size and steel fiber volume on fracture behavior of SCC were studied.
- The largest aggregate size of 12.5 mm can be appropriate for SCSFRC concrete.
- Fracture properties of SCSFRC were obtained using two different methods using Work fracture method and Size effect method.
- Size effect method can predict the peak load with a good precision for SCSFRC beams.

ARTICLE INFO

Article history:
Received 17 July 2017
Received in revised form 7 November 2017
Accepted 26 November 2017

Keywords:
Fiber reinforced concrete
Fracture energy
Steel fiber
Self-compacting concrete
Size effect

ABSTRACT

This research has studied the effects of maximum aggregate size of coarse aggregate and volume fraction of steel fibers on the parameters of self-compacting concrete fracture/brittleness. The laboratory program was implemented and the percent fiber and aggregate size were considered variable. Accordingly, 9 mix designs were prepared in 3 series based on 0.1, 0.3, and 0.5% steel fiber and three aggregate sizes (9.5, 12.5, and 19 mm) were considered in each fiber series. A total of 108 different-size notched beams were then prepared and fracture parameters were studied using Work Fracture Method (WFM) and Size Effect Method (SEM). Results have shown that in both methods, the largest aggregate size of 12.5 mm can be appropriate for self-compacting steel fiber-reinforced concrete(**SCSFRC**), although it is more significant in work fracture method. With the increase of aggregate size to 19 mm, G_F and L_{ch} decrease in work fracture method. However, in size effect method the concrete will be more ductile if V_f is increased, and it will be more brittle if d_{max} is increased. Comparing to the size effect method, the work fracture method performed better in energy absorption with the increase of both aggregate size and the steel fiber percentage. Size effect in such concrete with different fiber percentages was as anticipated and G_f/G_f ratio was found 8.89.

1. Introduction

Nowadays, concrete is a very important and highly applicable material in industry and its ductility and ductility in mold and its strength variations with varying percentages of cement, aggregate, water, and additives have made it a very popular material for designers. However, it has weaknesses as well; low tensile strength, post cracking potential, brittleness/ductility, fatigue capacity, and impact strength are among the ones that need enhancement.

To improve some of the above mentioned weaknesses, use of fiber in concrete has become quite popular and fiber concrete is now widely used in the construction of sidewalks, roads, parking lots, airports, and tunnels [1,2]. Using steel fibers in concrete (SFRC) improves its tensile and bending strength, energy absorption, and ductility, but the effect depends on the type, volume, direction, and distribution of fibers in the fracture surface [3–5]. These **SFRC** features can play important role in the structure's economical concrete technology and materials; energy absorption and concrete reinforcement can effectively reduce concrete fracture risk [6].

Self-compacting concrete has good workability; it flows easily between reinforcement bars in the mold under its own weight without aggregate segregation and needing any vibration [7]. Using steel fibers in self-compacting concrete (SCSFRC) and studying its details have been reported by many researchers. Siddique et al. [8] showed that in fly ash-improved self-compacting concrete (SCC), an increase volume fraction hooked-ends steel fibers will increase tensile and bending strength of **SCC** with 0.5 and 1% steel

* Corresponding author.
E-mail address: mrghasemi@eng.usb.ac.ir (M.R. Ghasemi).

https://doi.org/10.1016/j.conbuildmat.2017.11.141
0950-0618/

fiber can have an acceptable workability. Beygi et al. [6] studied the effects of three types of fibers (steel fibers, propylene, and glass) and nano-silica on **SCC** and showed that an optimal use of fibers and nano-silica can improve its mechanical properties; Ferra et al. [9] reported similar results too. Madandoost et al. [10] studied the mechanical behavior of SCC under the effects of varying cements (400, 450, and 500 Kg/m^3) and different steel fiber percentages ($V_f = 0$, 0.38, 0.64, and 1%) with two maximum aggregate sizes ($d_{max} = 10$ and 20 mm) and showed that an increase of d_{max} increased the compressive strength, but an increase in the fiber volume decreased it. Alberti et al. [11] showed that in normal vibrated concrete (NVC) and **SCC** reinforced with polypropylene fibers 60 mm long, an increase in fiber reduced compressive strength and modulus of elasticity, but increase the tensile strength.

A change in any concrete element such as aggregate size, volume, type, cement, and water-cement ratio (W/C), or adding such additives as fly ash, nano-silica, or fiber can affect its mechanical, rheological, and specifically, its fracture behavior leading to a different crack behavior; this has been reported by many researchers [15–21]. Beygi et al. [15] showed that in **SCC**, an increase in aggregate size, increased fracture energy, characteristic length (L_{ch}) and length of fracture proses zone (C_f). They also stated when decrease water to cement ratio from 0.7 to 0.35 increase fracture energy, decrease L_{ch} from 427 to 251.1 mm and C_f from 29.1 to 14.1 mm [20]. Karamloo et al. [19] studied the effects of aggregate size in self-compacting concrete with light aggregates (SCLC) and showed that an increase in size increased the **SCLC** fracture energy. Alyahya et al. [21] reported similar results too and showed that an increase in aggregate size increased the fractal dimension.

In fiber reinforced concrete, cement and aggregate size/volume are not the only parameters that affect the properties of the newly hardened concrete; length, diameter, type, length-to-diameter ratio (l/d), and amount of fiber too play vital roles [10]. Adding fiber to cement matrix prevents the crack growth and makes the matrix more ductile; since concrete brittleness is a measurable parameter (when effect of size is studied), adding fibers can vary this parameter.

Size effect shows its importance when one attends to interpret the behavior of real structures through small laboratory prototypes. Since the affected area of the crack tip can have linear or nonlinear behavior depending on the structure size, Bazant proposed some specific criteria (low-size effects) needed for such studies [22,23]. Researches on size effects and fracture energy are many [15,19,20], but those performed in recent years show that adding fiber to concrete affects all the features of the newly hardened concrete and require more studies. Yoo et al. [24] showed that using fiber in high strength concrete reduces size effect compared to **NVC**. Sahin & Koksal [25] studied the effects of different fiber types and volumes on high strength concrete and concluded that fiber volume had considerable effect on the tensile strength and characteristic length parameter.

This research aims to study the fracture parameters of self-compacting steel fiber-reinforced concrete and to show that adding steel fibers to the latter as a new material in the mix design will vary the fracture matrix and will cause changes in the fracture energy; in other words, we are going to study the fracture energy variations with the changes in maximum aggregate size (d_{max}) and volume fraction of fiber (V_f) in **SCC** which is flow-able, does not need vibration, and fiber distribution in it is quite random. Studies and their related results have revealed that information on the use of fiber in **SCC** is still insufficient and more studies are required in this regard. This paper has analyzed the fracture parameters using size effect method and work fracture method in a laboratory work.

2. Calculating fracture parameters

2.1. Work fracture method

For the first time, Hilerborg [26] proposed the fictitious crack model wherein the fracture energy (G_F) is found as follows:

$$G_F = \frac{\int Pds}{b(w-a)} \tag{1}$$

where a is the initial crack length in the beam under three-point bending, w is the specimen width, b is its thickness, and $\int Pds$ is the total area under load–displacement curve. Earlier studies [10,11] have shown that adding fibers can hardly enhance the compressive strength (it sometimes even reduces it), but the main reason for this adding is to improve the concrete post cracking ductility strength behavior. Accordingly, to better indicate the fiber concrete behavior and energy absorption, notched beams based on RILEM TC-189 SOC [27], ASTM 1609 [28], and RILEM TC-50 FMC recommendations [29] have been used.

To show the material brittleness or ductility, Hilerborg introduced another parameter called characteristic length (L_{ch}) as follows:

$$L_{ch} = \frac{EG_F}{f_t^2} \tag{2}$$

where E is the modulus of elasticity, f_t is the tensile strength, and G_F is the fracture energy. A high L_{ch} is an indication of concrete ductility and higher crack strength and vice versa.

2.2. Size effect method

Using the fracture parameters for concrete and semi-brittle materials, Bazant and Pfeiffer [22] presented the size effect theory through a specific method as follows:

$$\sigma_N = \frac{B}{\sqrt{1+\beta}} \qquad \beta = \frac{d}{d_0} \tag{3}$$

where β (introduced by Bazant-Kazemi [23]) shows the brittleness number and B and d_0 are experimental parameters found as follows using regression analyses and considering the peak load for different-size specimen:

$$\begin{aligned} &Y = AX + C \\ &X = d \quad Y = \left(\frac{1}{\sigma_N}\right)^2 \quad d_0 = \frac{C}{A} \quad B = \frac{1}{\sqrt{C}} \end{aligned} \tag{4}$$

Considering the above relations, such parameters as fracture energy (G_f), effective length of process zone (C_f), and fracture toughness (K_{IC}) can be determined as follows:

$$G_f = \frac{g(\alpha_0)}{AE} \tag{5}$$

$$C_f = \frac{g(\alpha_0)}{\acute{g}(\alpha_0)}\frac{C}{A} \tag{6}$$

$$K_{IC} = \sqrt{E\,G_f} \tag{7}$$

where $g(\alpha_0)$ and $g'(\alpha_0)$ are dimensionless equations of the rate of energy release, and A is the slope of line found by regression. All the above relations are fully presented in RILEM TC 89 [30] where in notched beams under three-point loading have been used and the mold width (b) is recommended must not be less than 3 times the largest aggregate size, but in ASTM 1609 [28], it is recommended that b should be at least 3 times the fiber length. Since

self-compacting concrete is quite flow-able and lies in the mold without vibration, random distribution [31] of steel fibers should be possible in the mold; therefore, in this research, a mold width (b) is the same for all the specimen, b = 100 mm.

3. Experimental framework

3.1. Materials

Materials used include Type II Portland Cement of Sistan Cement Factory (Zahedan, Iran) with physical/chemical specifications as shown in Table 1, natural sand fine aggregates with a fineness modulus of 2.8, natural crushed gravel coarse aggregates of maximum sizes 9.5, 12.5, and 19 mm with a specific weight of 2.93, super plasticizer with polycarboxylate base modified for steel fiber concrete to reach the flow-ability required by the EFNARC [13], low strength hooked-ends steel fibers (Table 2), W/C = 0.55 for all the specimens, and ultra-fine limestone powder to modify viscosity of the mixtures.

3.2. Mix designs

To study the fracture parameters in **SCSFRC**, the percent fiber and maximum aggregate size were considered variable and, accordingly, nine mix designs were prepared in 3 series based on V_f = 0.1, 0.3, and 0.5% fiber and three aggregate sizes (d_{max} = 9.5, 12.5, and 19 mm) were considered in each fiber series. A constant W/C ratio (0.55) and aggregate weight were considered in all these mixes so that only the effects of percent fiber and aggregate size may be observed. Mix designs, aggregate sizes, and fiber percentages have been selected based on the related papers available in the literature and complete specifications of the 9 mix designs are shown in Table 3 [6,10,15,19].

3.3. Specimens: Preparation and testing

This experimental plan has been designed to find the effects of maximum aggregate size (d_{max}) and fiber volume (V_f) on fracture energy and hence different-size notched beams were tested under three-point bending conditions (Fig. 1). As mentioned before, Beams sizes were selected based on RILEM [30] to determine the fracture parameters by size effect method (Fig. 2). In this recommendation, beam dimension b is selected based on d_{max}, but sometimes in fiber concrete the fiber length is more than d_{max} and hence in the ASTM 1609 [28] the beam dimension b should be selected at least 3 times the fiber length. Therefore, considering the self-compacting concrete flow-ability, and to prevent disturbance in fibers random distribution, the mold width (b) in this study was taken equal to 100 mm constant for all the specimens; other beam parameters such as $L/d, S/d$, and a_0/d were 2.67, 2.5, and 0.2 respectively (Table 4) based on the RILEM recommendation [30].

To determine the effects of d_{max} and V_f on fracture parameters by work fracture method, use was made of 350 × 100 × 100 mm^3 notched beams tested with span equal to 300 mm under three-point bending conditions (Fig. 1) according to ASTM 1609[28] and RILEM TC-187 [27]. In both methods, the notch width was 0.3 mm created by acrylic plates, and to measure the modulus of elasticity, splitting tensile strength, and compressive strength, six 15 × 30 mm standard cylinders were made. After being prepared, all specimens were kept in their molds in the laboratory for 24hr and then transferred (after molds were opened) to a water tank with a temperature of 20 ± 2 °C and kept there for 28 days. The compressive strength (f_c), modulus of elasticity (E), and splitting tensile strength (f_t) were found according to BS EN 12390 [34], ASTM C469 [14], and ASTM C496 recommendation [13]. Fresh concrete tests such as slump flow, flow time, L-box, and sieve test were done (Table 3) according to EFNARC [12].

Table 1
Portland cement type Π chemical and physical properties.

Chemical analysis		Results
SiO_2(%)		21.05
Al_2O_3(%)		4.76
Fe_2O_3(%)		3.43
CaO(%)		62.86
MgO		3.46
SO_3		1.87
Na_2O(%)		0.21
K_2O(%)		0.58
CL		0.04
$LO.I$(%)		1.2
$I.R$(%)		0.53
C_3S(%)		53.4
C_2S(%)		20.1
C_3A(%)		6.9
C_4AF(%)		10.4
$F.CaO$(%)		3.2
Physical Test		
Blaine(cm^2/kg)		3110
Setting Time (min)	*initial*	183
	Final	238
Autoclave.Exp(%)		0.08
Comp.Streng (MPa)	3 Day	26.5
	5 Day	45.1

Table 2
Properties of hooked-end steel fiber.

Length (mm)	30
Diameter (mm)	0.6
Aspect ratio (l/d)	50
Density(Kg/m^3))	7850
Tensile strength, f_{su}(N/mm^2)	1200

4. Results and discussion

4.1. Work fracture method

Fracture energy and characteristic length parameters can be found by relations (1) and (2) presented in RILEM 50FMC [29]. In work fracture method, G_F equals the area under load–displacement curve found through the three-point bending tests on notched beams discussed in Sec. 2. G_F variations with d_{max} changes in both **NVC** and **SCC** have been reported by many researchers. In their recent study, Beygi et al. [15] have shown that in **SCC**, when d_{max} increases from 9.5 to 19 mm, G_F reaches from 114.2 to 152.2 and from 107.3 to 144.2 N/m for W/C ratio of 0.38 and 0.53 respectively. Similar to other researchers, they attributed the G_F increase (due to d_{max} increase) to the complexity of the crack route and fractal dimension, and concluded that when d_{max} increases, more energy is absorbed; results of this research (shown in Table 5 and Fig. 3) show that G_F depends on d_{max} and when the latter increases from 9.5 to 12.5 mm, there is an increasing trend and from 12.5 to 19 mm, the trend is decreasing. The reason for this phenomenon is that with the increase of maximum aggregate size, fibers have less space for rotation and movement (Fig. 4). The best form for fiber placement on the fracture surface is horizontal (perpendicular to it). But at d_{max} = 19 mm, fibers are more inclined (angled) or are perpendicular (parallel to the fracture surface – Fig. 4) [32]. When fibers are more angled at the fracture surface, they lose their efficiency and help the growth of micro-cracks on the fracture surface meaning its disruption and, hence, a reduction in the fracture energy.

Table 3
Mix proportion of concrete series and fresh properties.

Materials		Weight (kg/m^3)								
		Seri 1			Seri 2			Seri 3		
		SCSFRC1	SCSFRC2	SCSFRC 3	SCSFRC 4	SCSFRC5	SCSFRC 6	SCSFRC 7	SCSFRC 8	SCSFRC 9
Cement (C)		375	375	375	375	375	375	375	375	375
Steel fiber (V_f%)		0.1	0.1	0.1	0.3	0.3	0.3	0.5	0.5	0.5
Sand		846	846	846	846	846	846	846	846	846
Coarse aggregate	4.75–9.5 (mm)	750	300	300	750	300	300	750	300	300
	9.5–12.5 (mm)	–	450	300	–	450	300	–	450	300
	12.5–19 (mm)	–	–	150	–	–	150	–	–	150
Limestone powder		180	180	180	180	180	180	180	180	180
Free water(W)		195	195	195	195	195	195	195	195	195
Superplasticizer(kg)		3	3	3	3.75	3.75	3.75	4.5	4.5	4.5
Unit weight (kg/m^3)		2340	2320	2400	2200	2260	2320	2257	2295	2360
Flow time(sec)		2.98	2.80	2.85	3	2.6	2.98	3.01	2.88	3.45
Slump flow(mm)		600	650	670	590	715	655	630	670	690
L-Box(h_2/h_1)		0.83	0.86	0.9	0.82	0.88	0.83	0.81	0.85	0.89
Sieve test (%)		1	1	1.3	1	2.9	1	1.2	1	1.2
W/C (by weight)		0.52	0.52	0.52	0.52	0.52	0.52	0.52	0.52	0.52

Fig. 1. Test setup of specimens with d = 200 mm (Left), specimens with variation size (Right).

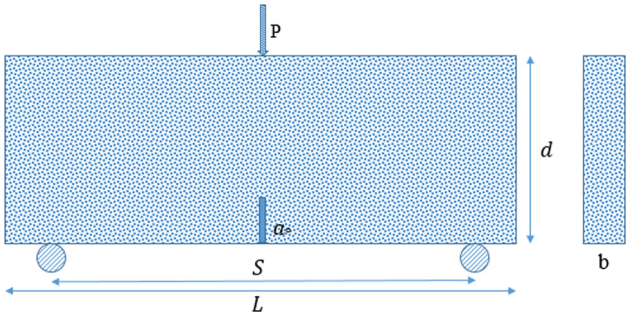

Fig. 2. Geometry of the three-point bending specimen.

Earlier researches have shown that when V_f increases, the modulus of elasticity and compressive strength show contradicting behavior [22,25]. The reasons can be: 1) when V_f increases, the compressive strength may decrease depending on how fibers are distributed; in high volumes, fibers may be aligned with the applied force and act like voids which are the starting points for micro cracks that cause strength drop reduction in concrete and 2) it is possible that fibers may be accumulated in one point due to improper distribution in the mold and cause micro cracks to begin from this concentration point. Fig. 3 shows that when d_{max} increases from 12.5 to 19 mm, G_F decreases; it can be stated that fibers and large aggregates cause improper fiber distribution and disturbance in the materials and commencement of more micro cracks that cause the energy absorption to reduce.

Koksal & Sahin [25] studied fracture energy for high strength concrete, used V_f = 0.33, 0.67, and 1% hooked-ends steel fibers, and showed that an increase V_f led to an increased G_F. Aberti et al. [11] have reported that in **SCC** with propylene fibers, an increase in the fiber volume increased G_F from 152 to 5420 (Fig. 3 shows the same idea without considering d_{max}). By forming a bridge between the two crack ends, fibers prevent its growth and hence

Table 4
Determination of beam specimen in size effect method.

Aggregate size (mm)	Steel fiber Length (mm)	d (mm)	b (mm)	a_0/d	S/d	L/d
9.5, 12.5, 19	30	100 200 400	100	0.2	2.5	2.67

Table 5
Value of *GF* measured from beam tested in mixtures.

MIX ID	Steel fiber (V_f) (%)	f'_c (MPa)	E (GPa)	f_t (MPa)	Average G_F(N/m)	Average L_{ch} (mm)
SCSFRC1	0.1	32.4	27.54	3.5	226.19	492.53
SCSFRC2	0.1	24.55	26.95	3.13	317.51	873
SCSFRC3	0.1	25.49	28.055	3.28	249.25	647.35
SCSFRC4	0.3	26.15	23.03	4.17	367.910	485.7
SCSFRC5	0.3	27.55	24.48	3.58	483	922.55
SCSFRC6	0.3	27.41	27.13	3.85	463	844.51
SCSFRC7	0.5	23.75	20.19	3.22	480.48	935.63
SCSFRC8	0.5	22.55	23.91	2.93	647	1793.41
SCSFRC9	0.5	30.15	30.62	3.12	491	1395.11

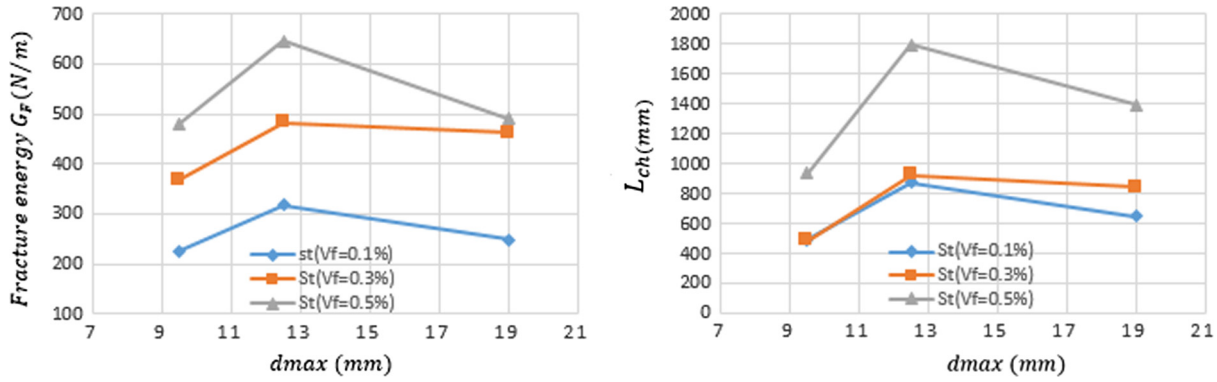

Fig. 3. Variation of the total fracture energy with maximum size of coarse aggregate (Left), Variation of the L_{ch} with maximum size of coarse aggregate (Right).

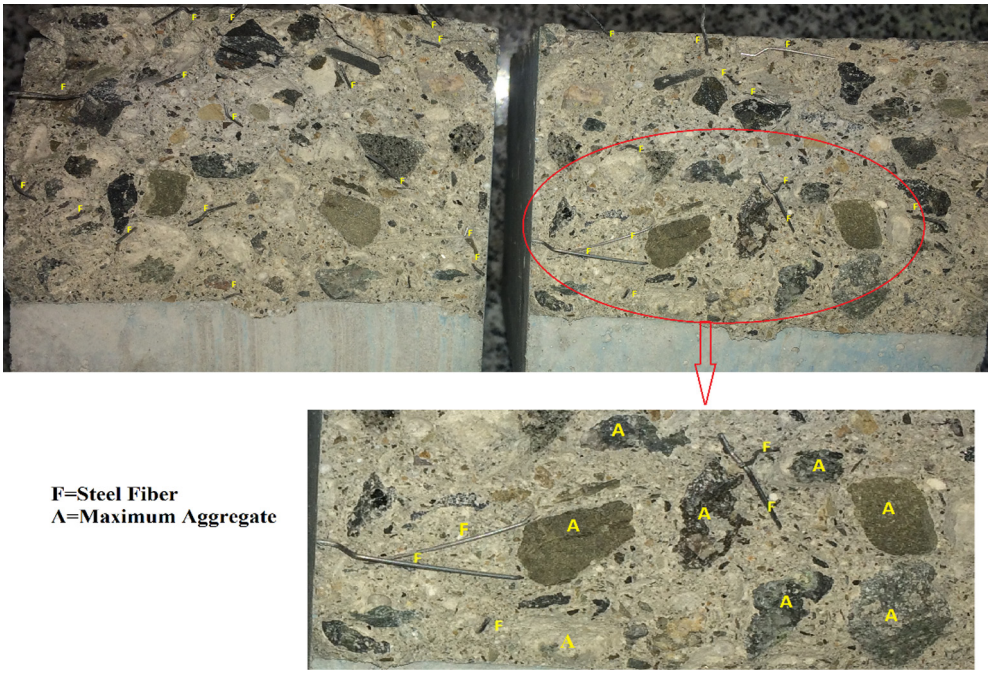

Fig. 4. Fracture surface with d_{max} = 19 mm.

energy absorption increases; of course fiber kind, type, and material can affect the amount. Results have also shown that when d_{max} increases from 9.5 to 12.5 mm, G_F curve is ascending, but from 12.5 to 19 mm, it is descending. The L_{ch}, which is an indication of brittleness in normal concrete, can also be used to determine the ductility of steel fiber concrete. Table 5 shows that with an increase in V_f, L_{ch} increases too meaning more concrete ductility. All in all, results in Fig. 3 show that steel-reinforced self-compacting concrete shows more energy absorption and ductility at d_{max} = 12.5 mm.

4.2. Size effect method

As mentioned in Section 2.2, relations 3–7 are used to determine fracture energy (G_f), length of process zone (C_f) and fracture toughness (K_{IC}) by size effect method. In this method, we only need to find the peak load (post peak is not required). Table 6 shows peak load for all different-size specimens under three-point bending test conditions. After finding the peak loads for all specimens using the linear regression, coefficients A and B are found according

Table 6
Corrected maximum loads for mixes.

MIX ID	$f'_c(MPa)$	a_0/d	Depth d(mm)	Corrected maximum load P_0 (N)		
				Beam 1	Beam 2	Beam 3
SCSFRC1	32.4	0.2	100	8058.5	8558.5	8258.5
			200	14234	13234	13034
			400	22836	21836	21936
SCSFRC2	24.55	0.2	100	7258	6458	7058
			200	13432	12732	13535
			400	19928	19728	–
SCSFRC3	25.49	0.2	100	7260	77760	6460
			200	11840	13540	17470
			400	20560	21960	21460
SCSFRC4	26.15	0.2	100	6655	7365	6855
			200	14455	12500	10900
			400	19980	20380	19280
SCSFRC5	27.55	0.2	100	7356.5	7396.5	7056
			200	12426	14226	12226
			400	21704	21104	18104
SCSFRC6	27.41	0.2	100	7258	7734	6858
			200	12737	12492	12232
			400	18828	18928	19328
SCSFRC7	23.75	0.2	100	6556.42	6756.42	5756.42
			200	12425.5	13525.7	12225.7
			400	17902.8	20402.8	18902.8
SCSFRC8	22.55	0.2	100	6757.37	7457.37	7057.37
			200	13429.5	13829.5	13229.5
			400	20518	21218	19918
SCSFRC9	30.15	0.2	100	8859	8656	8959
			200	16136	15136	15736
			400	22644	26144	23944

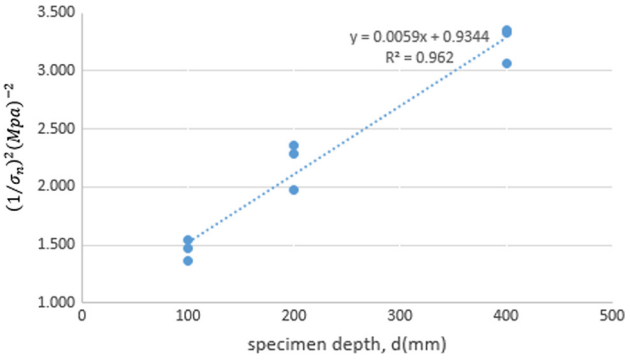

Fig. 5. Linear regression for size effect parameters.

to RILEM TC89 [30]; for this purpose, Fig. 5 shows the linear trend line for mix design **SCSFRC1**. In this Graph, slope of the fitted curve and intercept with the fitted line include $A = 0.0059$ and $C = 0.934$. Besides, according to RILEM, the coefficient of variations for intercept (w_c) and line slope (w_A) are respectively 0.156 and 0.0893.

Relative width of scattering band (m), slope coefficient variations and intercept should not exceed 0.2, 0.1, and 0.2 respectively; in this research most of the values lie in this range and differences, if any, are negligible. In size effect method, size range plays an important role in the reliability of results; the wider is the size range, the more reliable will be the results. Considering the dispersion of the size of specimens and properties of concrete, the minimum acceptable size range has been taken to be 1:4. The required main parameters such as G_f, C_f, and K_{IC} have been calculated and the results are shown in Table 7 and Fig. 6. Earlier researches show that the fractal dimension, and hence fracture toughness and fracture energy, increase with an increase in d_{max}. Beygi et al. [15] showed that in **SCC** with W/C of 0.38 and 0.53, when d_{max} increases from 9.5 to 19 mm, G_f increases from 20.14 to 28.4. Karamloo et al. [19] too showed that in **SCLC** with W/C of 0.35 and 0.4, when d_{max} increases from 9.5 to 19 mm, G_f increases from 25.5 to 36.26 and 16.9 to 31.5.

G_f and C_f are shown in Fig. 6 where at $d_{max} = 9.5$ and 12 mm, energy absorption increases with an increase in V_f, but at $d_{max} = 19$ mm, it seems that concrete shows a different behavior. The reason is that in the size effect method the load–displacement curve is used only up to the peak load (post peak is not considered) meaning that the fiber performance is not quite clear. Since fibers appear on the fracture surface with different orientations, negative effects on the fracture matrix are expectable; therefore, as shown in Fig. 6, concrete with $V_f = 0.1\%$ behaves close to fibreless concrete and at $d_{max} = 19$ mm it shows the highest energy absorption. But, at $d_{max} = 19$ mm, there is an increase in the energy absorption when V_f increases from 0.3 to 0.5% meaning that, ignoring the behavior at $dmax = 19$ mm with $V_f = 0.1\%$, an increase in V_f increases the energy absorption, but an increase in d_{max} reduces it (the reason for this reduction has been fully explained in Sec. 4–1). An increase in d_{max} reduces the space for fiber movement and rotation causing fibers to be inclined (at an angle) to the fracture surface which, in turn, results in more micro-cracks and disturbance in the fracture matrix. It should be noted that the interface transition zone (ITZ) quality has a direct effect on the peak load and energy absorption, and any disturbance in the fracture matrix can reduce the energy absorption. C_f is a parameter that shows the concrete brittleness. As shown in Fig. 6, concrete has different behavior at $d_{max} = 12.5$ and 19 mm with $V_f = 0.1\%$. As reasoned earlier, if these two cases are ignored, in this method too, the concrete will be more ductile if V_f is increased, and more brittle if d_{max} is increased.

Fig. 7 shows that the test-yielded peak load conforms well to that found from size effect method that uses fracture parameters. It can be observed that fracture parameters generated by each

Table 7
Fracture parameters obtained from the size effect method for mix.

Series	f_c(MPa)	E(GPa)	a_0/d	$g(\alpha_o)$	G_f(N/m)	C_f(mm)	B(MPa)	d_o(mm)	K_{IC}(MPa mm$^{0.5}$)	δ_c(mm)	ω_A	ω_c	m
SCSFRC1	32.4	27.54	0.2	7.28	45.069	30.29	1.034	159.23	35.23	0.0224	0.08	0.15	0.10
SCSFRC2	24.55	26.95	0.2	7.28	39.47	33.83	0.906	177.83	32.61	0.0224	0.17	0.27	0.20
SCSFRC3	25.49	28.05	0.2	7.28	49.142	49.25	0.855	258.87	37.13	0.0296	0.21	0.22	0.19
SCSFRC4	26.15	23.03	0.2	7.28	47.341	38.60	0.858	202.92	33.01	0.0284	0.19	0.26	0.20
SCSFRC5	27.55	24.48	0.2	7.28	42.55	30.55	0.943	160.621	32.27	0.0232	0.11	0.2	0.14
SCSFRC6	27.41	27.13	0.2	7.28	31.483	21.69	1.014	114.012	29.22	0.0160	0.05	0.12	0.07
SCSFRC7	23.75	21.2	0.2	7.28	53.70	38.94	0.857	202.44	32.94	0.0323	0.13	0.18	0.14
SCSFRC8	22.55	23.91	0.2	7.28	48.54	36.37	0.912	191.181	34.07	0.0366	0.16	0.24	0.18
SCSFRC9	30.11	30.62	0.2	7.28	47.69	27.67	1.174	145.456	38.21	0.0209	0.1	0.19	0.12

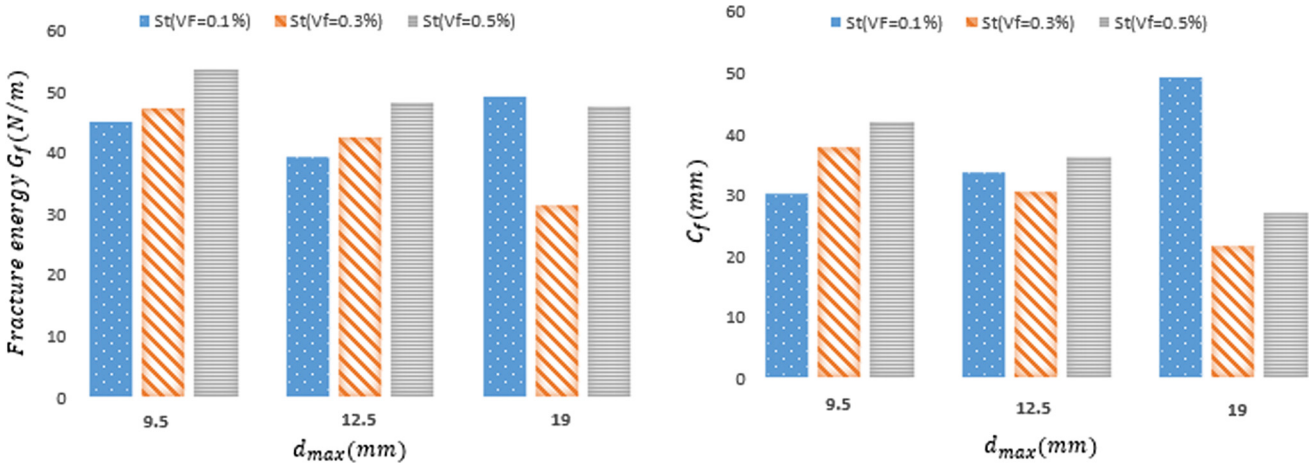

Fig. 6. Variation of the G_f (Left) and C_f (Right) from size effect method with maximum size of coarse aggregate for mixes.

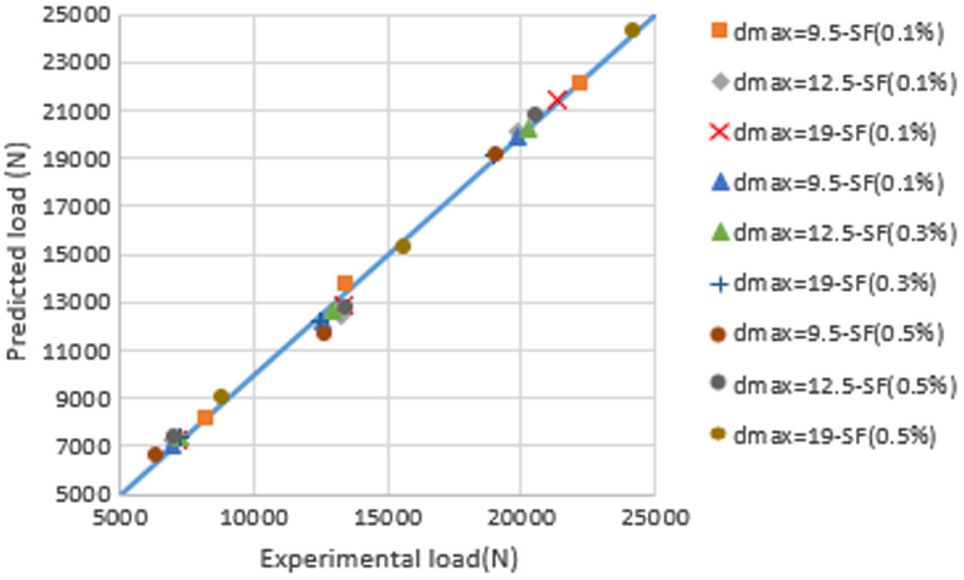

Fig. 7. Experimental and predicted peak load.

mix can be used to predict the fracture load of the self-compacting steel fiber-reinforced concrete. Fig. 8 shows the size effect graph fitted by the experimental data of the nine mix designs. It can be observed that the experimental data and prediction results found from size range conform (overlap) quite well.

Another important size effect method parameter is brittleness number (β) which is mostly used to find the fracture mode. Fig. 9 shows that for the nine mix designs with varying d_{max}, β lies in the nonlinear fracture mechanic range ($0.1 \leqslant \beta \leqslant 10$); when $\beta > 10$, rupture is to be found based on **LEFM** and when $\beta < 0.1$, analysis tends towards the strength criteria.

Altogether, it can be concluded that in the size effect method too, the fracture energy and ductility increase with an increase in V_f (not considering the maximum aggregate size), but they decrease when d_{max} increases from 9.5 to 19 mm. Results also show that the lowest C_f variation is 5% (related to d_{max} = 12.5 mm).

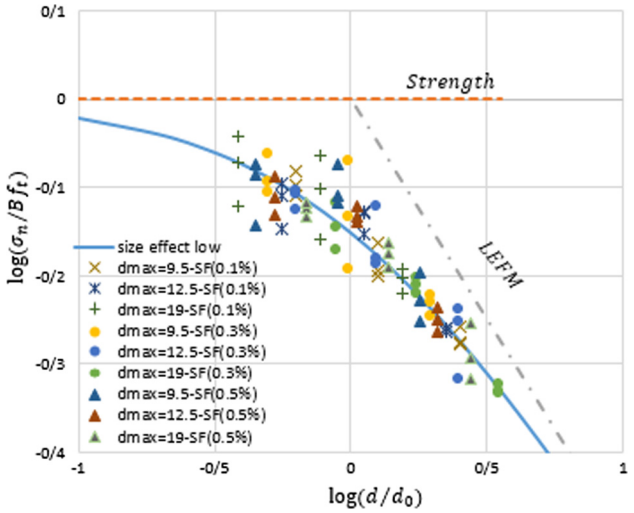

Fig. 8. Size effect plot of SCSFRC specimens with various maximum size of coarse aggregate.

5. Comparing fracture energy measured by two different methods

Fracture energy calculation by work fracture method and size effect method involves differences, the important ones of which are as follows:

1- In work fracture method, the whole area under load–displacement curve is used to calculate G_F while in size effect method only the initial slope of the softening curve is used; this is why G_F is always greater than G_f.
2- In size effect method, size effect is considered while in work fracture method only one specimen size is used.

Some researchers have shown that it is possible to define a relationship between the two energy values [23], but some believe that this relationship cannot be precise [33]. Reasons for this unreliability can be the G_F dependence on the specimen size, geometry, and testing process. The G_F/G_f ratios are shown in Table 8; the average

Table 8
Relationship between work fracture method and size effect method.

Steel fiber(V_f)(%)	*dmax*	G_F/G_f
0.1	9.5	5.018
0.1	12.5	8.044
0.1	19	5.072
0.3	9.5	7.771
0.3	12.5	11.348
0.3	19	14.706
0.5	9.5	7.788
0.5	12.5	9.986
0.5	19	10.295

G_F/G_f is 8.89 with a variations coefficient of 34%. In **SCSFRC**, an important point is the post cracking when fibers form a bridge, after crack formation, between the two crack ends and cause higher energy absorption and more ductility of the structure, but in size effect method, this important point is not observed. In Fig. 8, effect of size in **SCSFRC** is quite obvious and in Fig. 9 the nonlinear behavior of concrete is clear, but in work fracture method these points are not considered; therefore, it seems that in **SCSFRC** more research is needed for considering post cracking and size effect.

6. Conclusions

In this research, the fracture energy variations with changes in maximum aggregate size and the volume fraction of fiber were studied using work fracture method and size effect method and the following results were obtained:

- Results of both work fracture and size effect methods have shown that an increase in the maximum aggregate size and in the volume fraction of steel fiber, causes the fracture energy and parameters to change.
- In the work fracture method, increasing fibers in **SCC** can increase the energy absorption and ductility. But, increasing the largest aggregate size up to 12.5 mm can be beneficial to self-compacting fiber-reinforced concrete and result in more energy absorption. However, more increase in d_{max} than that can disturb the fracture matrix and reduce the energy absorption.

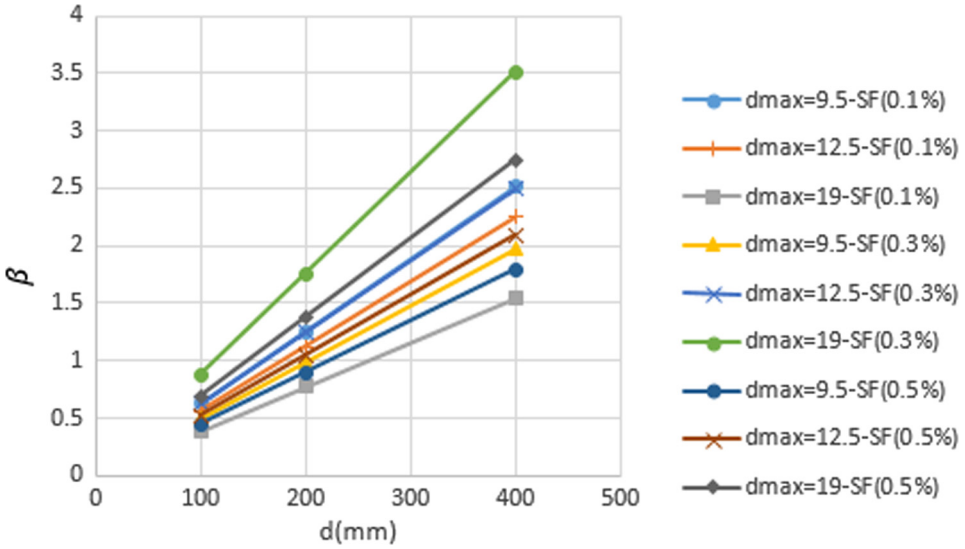

Fig. 9. Variation of brittleness number with depth.

- Since post cracking is not considered in the size effect method, V_f and fiber orientation on the fracture surface have direct impacts on the peak load. Results of this method show that an increase in d_{max} causes the concrete to show a more brittle behavior, but when V_f increases, the concrete becomes more ductile.
- Results show that at $dmax$ = 12.5 mm and different steel fiber percentages, the steel fiber-reinforced self-compacting concrete shows better behavior in both work fracture and size effect methods.
- Since fracture energy computation in work fracture method considers post cracking and the whole area under the load–displacement curve, it shows better results than size effect method.

References

[1] L. Sorelli, A. Meda, G.A. Plizzari, Steel fiber concrete slabs on ground: a structural matter, ACI Struct. J. 103 (4) (2006).
[2] A. Fuente, P. Pujadas, A. Blanco, A. Aguado, Experiences in Barcelona with the use of fibres in segmental linings, Tunnel. Underground Space Technol. 27 (2012) 60–71.
[3] P. Serna, S. Arango, T. Ribeiro, A.M. Nunez, E. Garcia-Taengua, Structural cast-inplace SFRC: technology, control criteria and recent applications in Spain, Mater Struct 42 (9) (2009) 1233–1246.
[4] R. Zerbino, J.M. Tobes, M.E. Bossio, G. Giaccio, On the orientation of fibres in structural members fabricated with self-compacting fibre reinforced concrete, Cement Concr. Compos. 34 (2) (2012) 191–200.
[5] L. Vandewalle, G. Heirman, F. Van Rickstal, Fibre orientation in self-compacting fibre reinforced concrete. In: Proc. of the 7th Int. RILEM Symp. on Fibre Reinforced Concrete: Des and Appl, (2008) 719–728.
[6] M. Beygi, J. Berenjian, O. Omran, A. Sadeghi Nik, I.M. Nikbin, An experimental survey on combined effects of fibers and nano-silica on the mechanical, rheological, and durability properties of self-compacting concrete, Mate Desi. 50 (2013) 1019–1029.
[7] Sh. Iqbal, A. Ali, A. Holschemacher, T.H. Bier, Mechanical properties of steel fiber reinforced high strength lightweight self-compacting concrete (SHLSCC), Constr. Build. Mater. 98 (2015) 325–333.
[8] R. Siddique, G. Kaur, Kunal. Strength and permeation properties of self-compacting concrete containing fly ash and hooked steel fibres, Constr Build Mater 103 (2016) 15–22.
[9] L. Ferrara, Y.D. Park, S.P. Shah, A method for mix-design of fiber-reinforced self-compacting concrete, Cem. Concr. Res. 37 (2007) 957–971.
[10] R. Madandoust, M.M. Ranjbar, R. Ghavidel, F. Shahabi, Assessment of factors influencing mechanical properties of steel fiber reinforced self-compacting concrete, Mate Desi. 83 (2015) 284–294.
[11] M.G. Alberti, A. Enfedaque, J.C. Galvez, Comparison between polyolefin fibre reinforced vibrated conventional concrete and self-compacting concrete, Constr. Build. Mater. 85 (2015) 182–194.
[12] EFNARC, The European Guidelines for Self-Compacting Concrete, Specification, Production and Use, (2005).
[13] ASTM C 496, Standard Test Method for Splitting Tensile Strength of Cylindrical Concrete Specimens, American Standards for Testing and Materials, 2011.
[14] ASTM C 469, Standard Test Method for Static Modulus of Elasticity and Poisson's Ratio of Concrete in Compression, American Society of Testing and Materials, 2004.
[15] M.H.A. Beygi, M.T. Kazemi, J.V. Amiri, I.M. Nikbin, S. Rabbanifar, E. Rahmani, Evaluation of the effect of maximum aggregate size on fracture behavior of self-compacting concrete, Constr. Build. Mater. 55 (2014) 202–211.
[16] F.E. Amparano, Y. Xi, Y.S. Roh, Experimental study on the effect of aggregate content on fracture behavior of concrete, Eng. Fract. Mech. 67 (1) (2000) 65–84.
[17] A. Hillerborg, Results of three comparative test series for determining the fracture energy GF of concrete, Mater. Struct. 18 (1985) 407–413.
[18] P. Acker, C. Boulay, P. Rossi, On the importance of initial stresses in concrete and of the resulting mechanical effects, Cem. Concr. Res. 17 (1987) 755–764.
[19] M. Karamloo, M. Mazloom, G.H. Payganeh, Effects of maximum aggregate size on fracture behaviors of self-compacting lightweight concrete, Constr. Build. Mater. 123 (2016) 508–515.
[20] M.H.A. Beygi, M.T. Kazemi, I.M. Nikbin, J.V. Amiri, The effect of water to cement ratio on fracture parameters and brittleness of self-compacting concrete, Mater. Des. 50 (2013) 267–276.
[21] W.S. Alyhya, M.S. Abo-Dhaheer, M.M. Al-Rubaye, B.L. Karihaloo, Influence of mix composition and strength on the fracture properties of self-compacting concrete, Constr. Build. Mater. 110 (2016) 312–322.
[22] Z.P. Bazant, P. Pfeiffer, Determination of fracture energy from size effect and brittleness number, ACI Mater. J. 84 (6) (1987) 463–480.
[23] Z.P. Bazant, M.T. Kazemi, Determination of fracture energy, process zone length and brittleness number from size effect, with application to rock and concrete, IJFr 44 (1990) 111–131.
[24] D.Y. Yoo, N. Banthia, J.M. Yang, Y.S. Yoon, Size effect in normal- and high-strength amorphous metallic and steel fiber reinforced concrete beams, Const. Build. Mater. 121 (2016) 676–685.
[25] Y. Sahin, F. Koksal, The influences of matrix and steel fibre tensile strengths on the fracture energy of high-strength concrete, Const. Build. Mater. 25 (2011) 1801–1806.
[26] A. Hillerborg, M. Modeer, P.E. Petersson, Analysis of crack formation and crack growth in concrete by means of fracture mechanics and finite elements, Cem Concr Res 6 (1976) 773–782.
[27] RILEM TC-187-SOC. Indirect test for stress-crack opening curve, (2007).
[28] ASTM C 1609/C 1690M-07. Standard test method for flexural performance of fiber reinforced concrete (using beam with third-point loading), (2007).
[29] RILEM FMC-50, Determination of the fracture energy of mortar and concrete by means of three-point bend tests on notched beams, Mater Struct 18 (4) (1985) 287–290.
[30] RILEM FMT-89, Size-effect method for determining fracture energy and process zone size of concrete, Mater. Struct. 23 (6) (1990) 461–465.
[31] A. Abrishambaf, V.M. Cunha, J.A. Barros, A two-phase material approach to model steel fibre reinforced self-compacting concrete in panels, Eng. Fract. Mech. 162 (2016) 1–20.
[32] L. Jiaping, L. Changfeng, L. Jiangzhong, D. Zhaojing, C. Gong, Characterization of fiber distribution in steel fiber reinforced cementations composites with low water-binder ratio, Ind. J. Eng. Mater. Sci. 18 (2011) 449–457.
[33] R.A. Einsfeld, M.S.L. Velasco, Fracture parameters for high-performance concrete, Cem. Concr. Res. 36 (2006) 576–583.
[34] BS EN 12390, Part 3: Testing Hardened Concrete. Method of Determination of Compressive Strength of Concrete Cubes, British Standards Institution, 2000.